東京大学 大学院新領域創成科学研究科
基盤科学研究系
先端エネルギー工学専攻

平成 24 年度

修士論文

Performance Evaluation of Reed Valve Air-Breathing System for Microwave Rocket

― マイクロ波ロケットのリード弁式吸気機構性能評価 ―

2013 年 2 月提出
指導教員　小紫　公也　教授

47116069　齋藤　翔平

Acknowledgement

I would like to express my gratitude to Professor Kimiya Komurasaki who gave me this research theme and many excellent advices. In addition, he has given me a lot of opportunities not only to do experiments but also to make presentations in many conferences. Without his instruction, my thesis could never be completed.

I am grateful to Professor Yoshihiro Arakawa (Department of Aeronautics and Astronautics) for his instructive advices and I've learnt attitude as a researcher or a student by his way.

I owe a huge debt to Associate Professor Hiroyuki Koizumi. He gave me a lot of meaningful advices. Especially, he gave advices for designing of microwave rocket thruster.

Dr. Keishi Sakamoto (Plasma Heating Technology Group, Naka Fusion Institute, Japan Atomic Energy Agency) gave our group some advices and the most precious opportunities of experiments including the opportunities to use a gyrotron, shield room, and so on.

Gratitude is also extended to the following members in the group; Dr. Koji Takahashi and Dr. Ken Kajiwara for cooperating experimental works and giving advices; Mr. Yukiharu Ikeda and Mr. Shinji Komori gave me warm support for conducting the experiment and helped me a lot including the preparation for the experiments (setup, instruments and operating the gyrotron).

The experiment could never be successful and my thesis could never be finished without Dr. Yasuhisa Oda. He gave me meticulous advices and direct instructions not only in the experiment but also even in the analysis of the data. Through these instructions, my way of thinking and working greatly improved. Therefore I would like to express my gratitude to him.

I thank to elders and betters at our laboratory at the University of Tokyo, Mr. Toshikazu Yamaguchi, Mr. Reiji Komatsu (Ministry of Education, Culture, Sports, Science and Technology) and Mr. Masafumi Fukunari, for their fruitful discussions. Especially, Mr. Reiji Komatsu always supported me a lot as the closest adviser for me. From him, I learned a lot of things, analysis of experimental data, treat of experimental instruments, way of better expression in my presentation. Many basic but indispensable knowledge of me came from him.

In addition, I am obliged for all members in Arakawa-Komurasaki-Koizumi lab, especially to Mr. Tensei Takeichi, Mr. Kenta Asai, Mr. Anthony Arnault and Mr. Satoshi Kurita, who gave me a lot of chances to make a discussion as the same research group. Furthermore, they supported me a lot in the experiment through their careful helps and warm words for me.

Finally, I would like to say "thank you" to my parents for infinite support.

Contents

Nomenclature

I : Impulse [Ns]

P_{peak} : Peak power of microwave beam [kW]

C_m : Momentum coupling coefficient [N/MW]

P : Average beam power [MW]

F : Average thrust [N]

T : Period of 1 engine cycle [s]

τ : Pulse duration time of microwave / 1 pulse [ms]

L : Thruster length [m]

f : Repetitive frequency of microwave [Hz]

U_{ioniz} : Propagation velocity of ionization front [m/s]

V : Output voltage from laser-displacement sensor [V]

V_0 : Amplitude of Output voltage from laser-displacement sensor [V]

U_s : Propagation velocity of shock wave [m/s]

σ_{Al} : Allowable stress of aluminum [MPa]

σ_{sus304} : Allowable stress of sus304 [MPa]

σ_y : Yield stress, proof stress [MPa]

f_{safety} : Factor of safety

σ_{max} : Maximum stress [MPa]

r : Inside diameter [mm]

p : Inside pressure [MPa]

t_{Al} : allowable thickness of aluminum [mm]

t_{sus304} : thickness of sus304 [mm]

y : Diaplacement of reed valve [mm]

I : Second moment of area [m^4]

E : Young's modulus [GPa]

M : Moment [Nm]

ρ : Density of reed valve [kg/m^3]

A : Section area [m^2]

λ_n : Mode of reed valve

ω_n : Natural frequency [Hz]

$A_{thruster}$: Cross sectional area of thruster [m^2]

$p_{plateau}$: Plateau pressure [MPa]

$t_{plateau}$: Plateau pressure maintained time [s]

$t_{1st\ plateau}$: Plateau pressure of 1st pulse maintained time [s]

$p_{1plateau\_reed}$: Plateau pressure of 1st pulse with reed valve [Pa]

$p_{1plateau\_no\ reed}$: Plateau pressure of 1st pulse without reed valve [Pa]

Chapter 1
Introduction

1.1 Current Circumstances of Space Transportation System

Recently, space development marked the end of human space explorations such as the Apollo program and it was changed for huge space facility such as ISS (International Space Station) or SSPS (Space Solar Power System). Consequently, low cost space transportation systems intended for large mass object is required rather than high cost space transportation systems intended for human such as space shuttle.

Most of present space transportation systems use chemical launcher rocket intended for not only human but also object. These rockets require huge costs and resources. For example, it costs around 10 billion yen to launch a typical satellite to GTO (Geostationary Transfer Orbit) [1]. There are mainly three reasons for these high costs as follows.

The first is that chemical rocket needs huge amount of propellant on board. About 90% of typical chemical rocket mass are occupied by fuel and oxidizer [2]. Therefore, the achievable payload ratio of chemical rocket is only several percent. As a result, launch cost of typical chemical rocket reaches about 1 million yen per 1 kg payload. In addition to this, chemical rockets need to produce high thrust because of its large mass include fuel. However the specific impulse of chemical rocket engines is limited only several hundred seconds. That is the why chemical rocket requires huge amount of propellant on board.

The second is that chemical rocket needs complex and expensive components such as turbo pump and high-pressure combustor. Chemical rocket needs these components in order to raise pressure of propellant and burn the fuel. In addition to these, a lot of pipes need in this system in order to connect these components. As a result, chemical rocket is complex, expensive and heavy.

The last is that chemical rocket can’t be reusable. Although chemical rocket needs complex and expensive components as mentioned before, it can’t be reusable. Therefore, chemical rocket is high cost and unfitted for large mass transportation to space.

As stated above, conventional space transportation system of chemical rocket is unfitted for large mass transportation to space. However, current development of space is required large mass transportation system to space. Therefore, Beamed Energy Propulsion (BEP) was suggested as one of the possible candidates.

1.2 Beamed Energy Propulsion (BEP)

In order to resolve high launch cost problem of conventional chemical rocket, beamed energy

propulsion (BEP) was suggested. Figure 1.1. shows schematic of BEP launching. The concept of BEP was suggested by Arthur Kantrowitz using laser launch system in 1972 [3]. BEP is the system which gains propulsive energy by high power beamed electromagnetic wave transmitted from outside of the thruster. Because BEP vehicles do not need to load an energy source, fuel tank, turbo pump, pipes or heavy electric source, the BEP vehicles structure can be quite simple. Furthermore, atmospheric air can be used as a propellant as long as the BEP vehicle flies in the atmosphere, the vehicle can achieve remarkably high payload ratio and specific impulse I_{sp}. In addition, because the energy beam station is built on the ground, it can be maintained easy and used during many launch counts. Therefore, the more the launch count, the more the development cost for a beam oscillator can be repaid.

The beam source is usually a high-power laser or microwave oscillator. In laser propulsion, various approaches to laser propulsion and laser launch were explored. A remarkable result is a launch demonstration conducted by Myrabo *et al*. achieving 71m launching [4]. On the other hand, for BEP using microwave, Knecht conducted an analysis on microwave thermal rocket system which propellant is heated by microwave, in 1980s [5]. Our research group also investigates microwave propulsion called as “Microwave Rocket” [6-8].

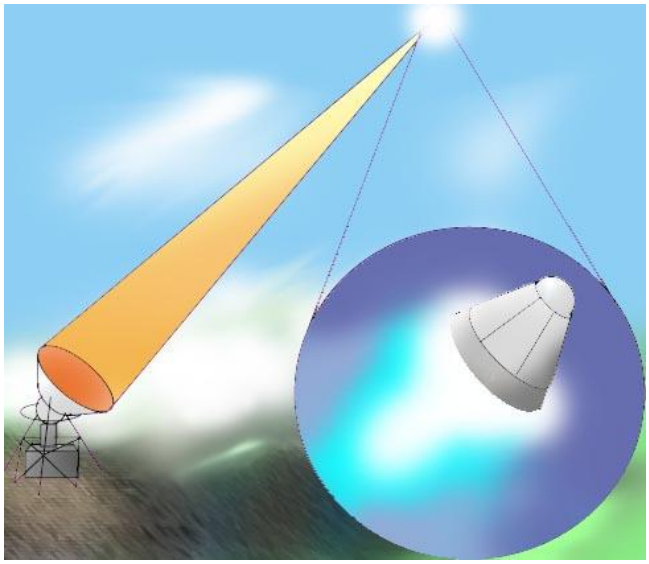

Figure 1.1. Schematic figure of beamed energy propulsion

1.3 Microwave Rocket

Compared with laser, microwave has some advantages as followings. Microwave generator is being developed in field of nuclear fusion as heat source of core plasma and has already realized 1MW class beam power and high energy conversion efficiency [9]. Furthermore its cost per beam power is 2 orders smaller than that of laser. Therefore, microwave rocket is proposed by our research group as the most promising idea to make it easy to exploration to the space.

1.3.1 Microwave Generator “Gyrotron”

A 1MW-class 170GHz gyrotron was used as a microwave source. Figure 1.2. shows the schematic of gyrotron. It was developed at Naka Fusion Institute of Japan Atomic Energy Agency (JAEA) for the Electron Cyclotron Heating and Current Drive (ECH&CD) system applied to International Thermonuclear Experimental Reactor (ITER). It can be operated under wide range of pulse duration (0.1 ms to 1000 s) and has achieved 50% energy conversion efficiency from electricity with Single-stage Depressed Collector as an energy recovery system. Its specifications are showed in Table 1.1.

The modulation method of gyrotron using anode-voltage modulation limited its peak power to 300kW because it was difficult to control spurious modes excitation during turn-off phase at high power operation. To increase peak power, a fast switching device composed of IGBTs (Insulated Gate Bipolar Transistor) which could turn on and off the beam current (100kV/30A) up to 5 kHz modulation was applied into the main driving circuits of gyrotron to stop the beam current during turn-off phase.

Figure 1.2. Schematic of gyrotron

Table 1.1. Specifications of gyrotron

Frequency	170GHz
Output Power P	< 1MW
Beam Profile	Gaussian
Beam waist	40mm
Electrical efficiency	50%

1.3.2 Engine Cycle of Microwave Rocket

Figure 1.3. shows the cross sectional view of microwave rocket with air-breathing system by reed valves. This rocket uses ram compression with an intake and reed valves [10]. A microwave beam irradiated from the ground is induced into a tapered reflector attached at the bottom of the thruster. The engine cycle of microwave rocket is illustrated in figure 1.4. The analogy of Pulse Detonation Engine (PDE) cycle is often used to explain this cycle [11]. As shown in figure 1.4., microwave rocket is operated by following cycle.

1. The cycle begins with air breakdown by focusing the high-power microwave beam pulse.
2. During microwave irradiation, a shock wave and an ionization front propagate together toward the open end of thruster. This process is called Microwave Detonation. The detonation wave is exhausted there. During this term, thrust is generated by high pressure inside a thruster.
3. An expansion wave propagates from the open end to the closed end.
4. When gauge pressure inside the thruster becomes negative by the expansion wave propagation, microwave rocket starts refilling with fresh air and prepares for the next cycle which begins with the next microwave pulse.

As above mentioned, during 2nd term of the engine cycle, thrust is generated by high pressure inside a thruster. Therefore, the longer high pressure generating time, the higher thrust is generated. Besides, at 4th term of the engine cycle, reed valves open and suction fresh air.

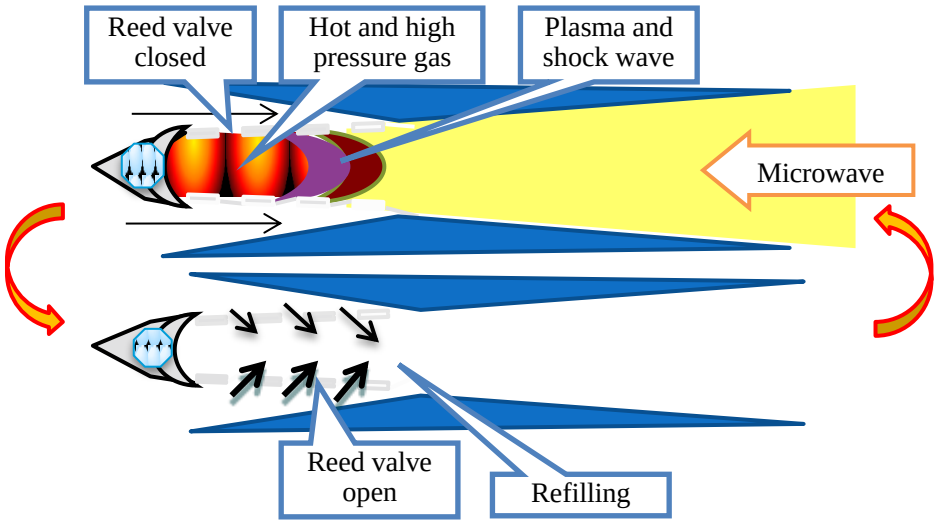

Figure 1.3. Cross sectional view of microwave rocket with air-breathing system by reed valves

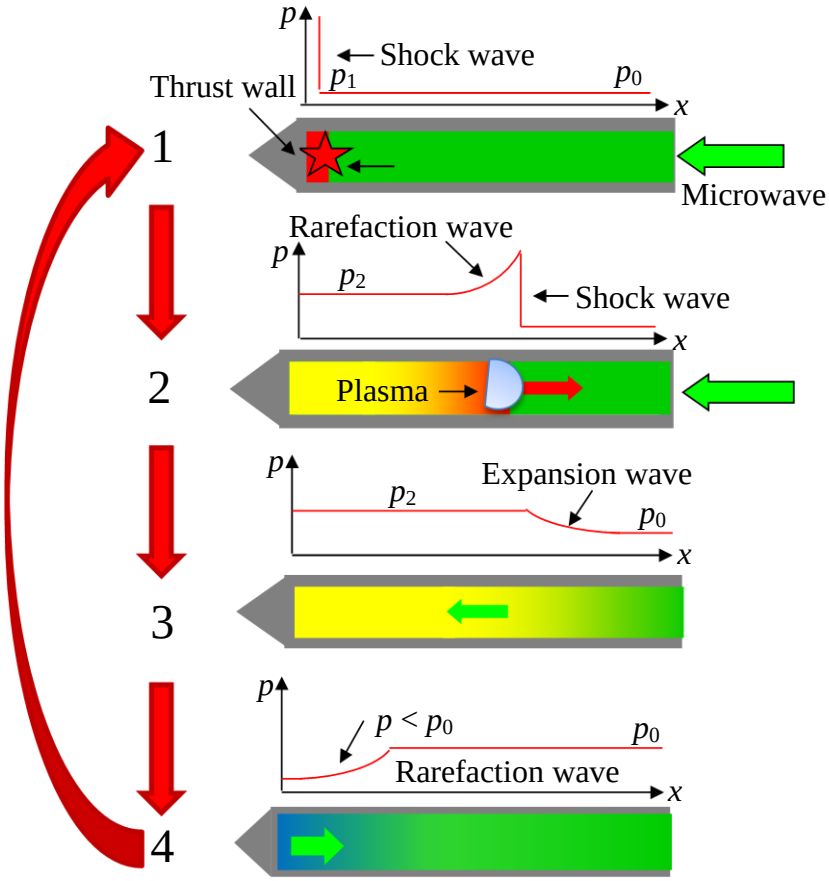

Figure 1.4. Engine cycle of microwave rocket

Chapter 2

Design of New Thruster

2.1 Characteristics of Microwave Rocket Thruster

Generally speaking, a thruster of BEP is quite simple. The shape of Repetitive Pulse (RP) laser propulsion thruster is like conical. The reason of this shape of thruster is that RP laser can be generated very high power, high repetitive frequency and short pulse duration time. Altogether, RP laser propulsion thruster has to ventilate in short interval because of its short cycle time. Therefore, the thruster is shaped like conical and RP laser make it possible to be generated high repetitive frequency. On the other hand, the shape of microwave rocket thruster is like cylinder. Compared with RP laser, microwave can be generated long pulse duration time by gyrotron. In order to maintain high pressure generating time inside the thruster due to long pulse duration time, the thruster of microwave rocket has to be shaped like cylinder.

Figure 2.1. Shape of RP laser propulsion thruster

Figure 2.2. Shape of microwave rocket thruster

2.2 Design of Main Body

A new thruster was designed. As mentioned above, one of the merits of microwave rocket is that high pressure generating time inside the thruster can be maintained in long time. Therefore, a thruster made of aluminum pipe was used in past study. And the size of this thruster (length, inside diameter and thickness) is 500 mm, 56 mm and 2 mm, respectively. In order to compare with past study data, a thruster of almost same size to past thruster is used in this study. Furthermore, in order to confirm the intensity of this thruster, it was calculated following.

Firstly, a new thruster is assumed thin cylindrical shell as figure 2.3. And pressure inside the thruster is assumed 0.5 MPa, because shockwave pressure measured pressure history is about 0.5 MPa.

Secondly, allowable stress was calculated as following. As a result, the thickness of thruster 2 mm is enough strong and can be used.

$$\sigma_{\mathrm{Al}} = \frac{\sigma_{\mathrm{y}}}{f} = \frac{110}{1.25} = 88\mathrm{MPa}$$

$$\sigma_{\max} = \frac{rp}{t}$$

$$\therefore \quad t_{\mathrm{Al}} = \frac{rp}{\sigma_{\mathrm{Al}}} = \frac{30 \cdot 0.5}{88} = 0.17\mathrm{mm}$$

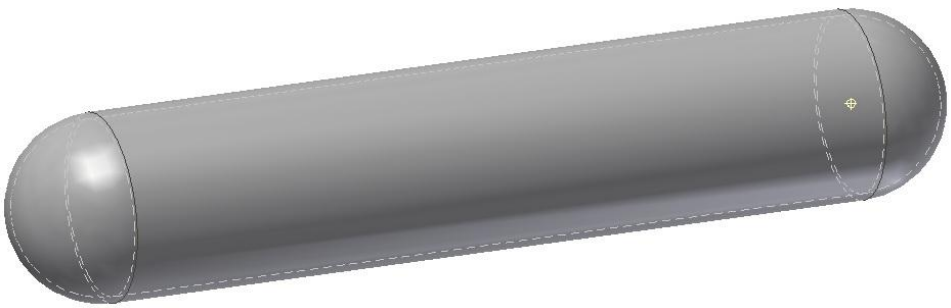

Figure 2.3. Assumed thruster model in order to design thruster

In past study, reed valve air-breathing system was attached only rectangular thruster because reed valve can be attached only flat surface. However, the beam shape of microwave is circle. Therefore, thruster was designed cylinder and reed valve was attached this thruster.

Figure 2.4. shows how to attach reed valve on cylindrical thruster. As shown in figure 2.4., reed valve can be attached on cylindrical thruster by part of reed valve attachment. In addition to this, it can be changed the number of reed valve by changing the number of the attachment. Followings are characteristics of the new thruster with reed valve air-breathing system.

- ✓ Part of reed valve attachment in order to attach reed valve on cylindrical thruster
- ✓ Rubber sheet in order to seal
- ✓ Reduce weight
- ✓ The number of reed valve can be changed
- ✓ Standard product is used in order to be cheap

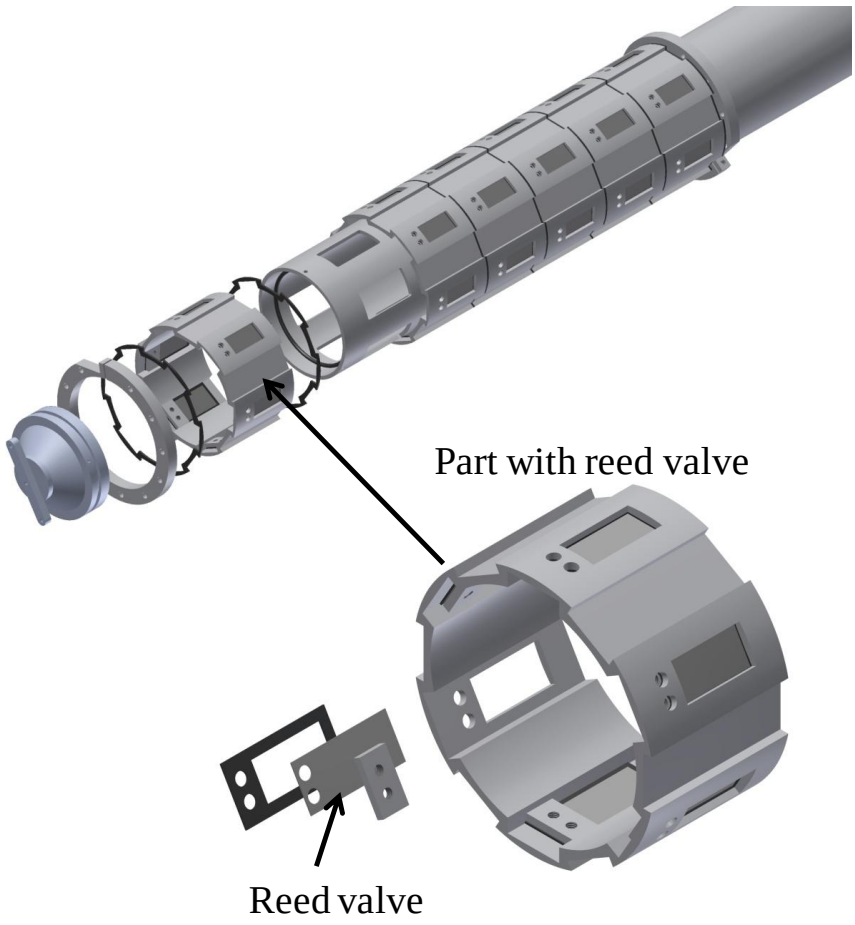

Figure 2.4. How to attach reed valve on cylindrical thruster

2.3 Design of Reed Valve

As mentioned above, microwave rocket needs to be refilled efficiently by reed valve air-breathing system. Hence, the size of reed valve needs to be designed along with thruster body. The size (length and width) and material of reed valve was decided in past study. Therefore, these are used same. However, the thickness was designed in this study, because it can be changed.

Firstly, allowable stress was calculated as following. As a result, if the thickness of reed valve were over 0.09 mm, reed valve can be used.

$$\sigma_{\mathrm{SUS304}} = \frac{\sigma_{\mathrm{y}}}{f} = \frac{200}{1.25} = 160\mathrm{MPa}$$

$$\sigma_{\max} = \frac{rp}{t}$$

$$\therefore \quad t_{\mathrm{SUS304}} = \frac{rp}{\sigma_{\mathrm{SUS304}}} = \frac{30 \cdot 0.5}{160} = 0.09\mathrm{mm}$$

However, plastic deformation occurred in present experiment discussed further below. Figure 2.5. shows relationship between impulse and each thruster (with reed valve and without reed valve). As shown in figure 2.5., impulse of with reed valve is smaller than without reed valve. The reason for this is that plastic deformation of reed valve due to reed valve opened too much. And the intensity calculation mentioned above was considered only high pressure inside thruster. Therefore, bending strength was considered in addition to calculation above. The method is following.

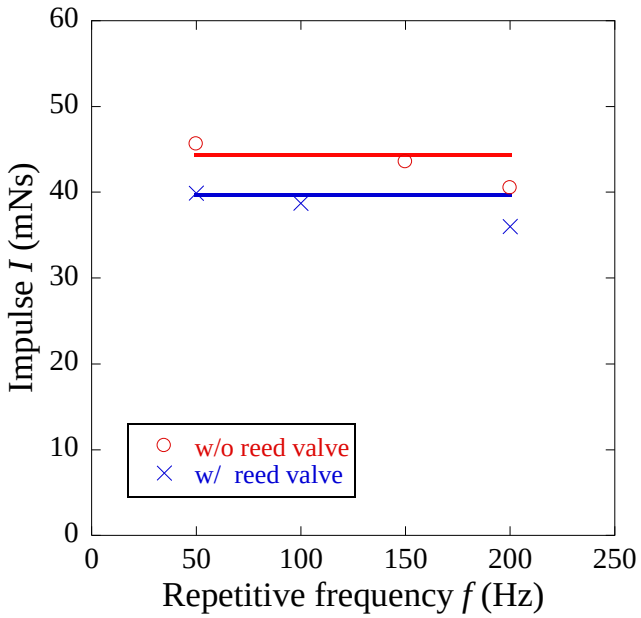

Figure 2.5. Impulse decrement due to plastic deformation

Three methods are used in this calculation.

First is calculation of cantilever bending as figure 2.6. As shown in figure 2.6., reed valve bends due to uniform load (negative pressure) and balances. Namely, displacement of reed valve is calculated by solving following differential equation.

$$\frac{d^2y}{dx^2} = -\frac{M}{EI}$$

$$y = \frac{p}{2EI}\left(\frac{x^4}{12} - \frac{L}{3}x^3 + \frac{L^2}{2}x^2 - \frac{l^3}{3}x + \frac{l^4}{12}\right)$$

$$\omega_n = \left(\frac{\lambda_k}{L}\right)\sqrt{\frac{EI}{\rho A}}$$

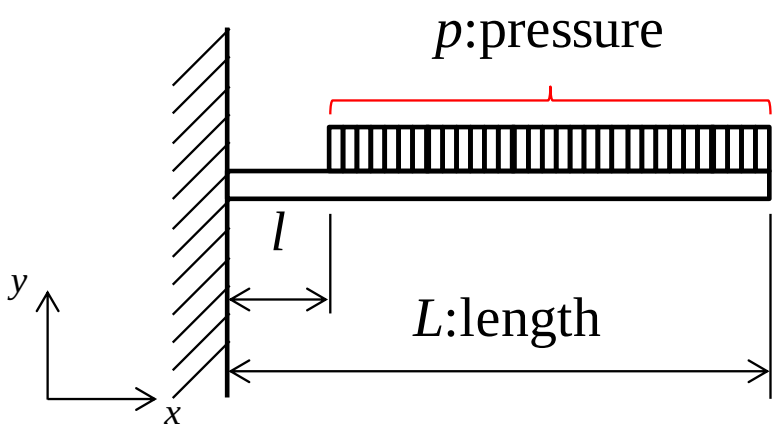

Figure 2.6. Model of cantilever bending calculation

Second is calculation used spring-mass system of Bernoulli-Euler beam. Figure 2.7. shows model of this calculation. This calculation is assumed that damping ratio of reed valve can be ignored and a spring is attached at the front of reed valve. Following equation of motion can be solved by this assumption.

$$\rho A \frac{\partial^2 y(x,t)}{\partial t^2} + EI \frac{\partial^4 y(x,t)}{\partial x^4} = 0$$

Concretely, the solution of this equation is assumed as following.

$$y(x,t) = \sum_i Y_i(x) q_i(t)$$

$$Y_i(x) = \cosh \lambda_i x - \cos \lambda_i x - \sigma_i (\sinh \lambda_i x - \sin \lambda_i x)$$

$$\sigma_i = \frac{\sinh \lambda_i l - \sin \lambda_i l}{\cosh \lambda_i l - \cos \lambda_i l}$$

$$\frac{\partial^2 q(t)}{\partial t^2} + 2\omega \xi_{eff} \frac{\partial q(t)}{\partial t} + \omega^2 q(t) = \omega^2 G(y) \Delta P$$

$$G = \frac{1/l \left[B(y) \int_0^l Y dx \right]}{\rho A \left[\int_0^l Y^2 dx \right] \omega^2}$$

Damping ratio is ignored. And the following equation derived.

$$\frac{\partial^2 q(t)}{\partial t^2} + \omega^2 q(t) = \omega^2 G(y) \Delta P$$

$$\frac{\partial^2 q(t)}{\partial t^2} = \frac{\left[B(y) \int_0^l Y dx \right]}{\rho b h l \left[\int_0^l Y^2 dx \right]} \Delta P - \left[(\lambda_i l)^2 \sqrt{\frac{EI}{\rho A l^4}} \right]^2 q(t)$$

$$\frac{\partial^2 q(t)}{\partial t^2} = \frac{\phi \cos \theta}{\rho h} \Delta P - E_c \frac{h^2}{b l^3} q(t)$$

$$R = \frac{\cos \theta}{h} \Delta P - \frac{\rho}{\phi} E_c \frac{h^2}{b l^3} q(t)$$

And, it is assumed to balance between left-hand member and right-hand member.

$$l = \sqrt[3]{\frac{\rho E_c y}{\phi Y \cos \theta b \Delta P}} h$$

Therefore, the thickness of reed valve is calculated by using this equation.

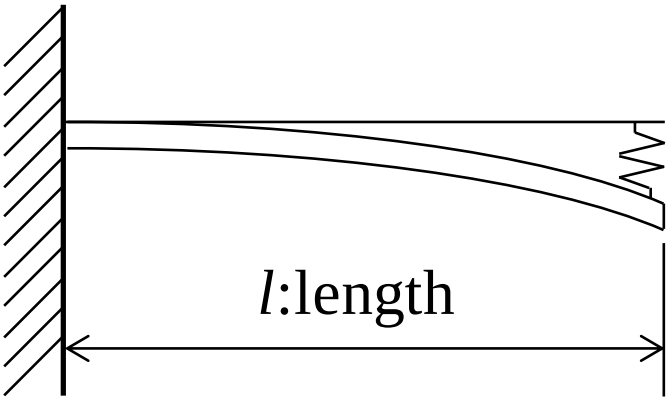

Figure 2.7. Model of Bernoulli-Euler beam calculation

Third is calculation used dynamic analysis [12]. Figure 2.8. shows model of this calculation. As shown in figure 2.8., $w(x, t)$ is displacement of reed valve. Therefore, following formulas are derived.

$$T = \frac{1}{2}\int_0^l \rho A(x)\dot{w}^2 dx$$

$$U = \frac{1}{2}\int_0^l EI(x)\ddot{w}^2 dx + \frac{1}{8}\int_0^l EA(x)\dot{w}^4 dx$$

$$W = \beta A_e \Delta p w \delta(x - l_1)dx$$

And, following equation of motion is derived from these formulas.

$$w(x,t) = \phi(x)q(t)$$

$$\phi(x) = x^4 - 4lx^3 + 6l^2x^2$$

$$\ddot{q} + 2\zeta\omega_n\dot{q} + \omega_n^2 q + \eta q^3 = f(t)$$

$$f(t) = \frac{\beta\Delta p}{m} \cdot \frac{bl^2\phi(l_1)}{2\sqrt{l_1^2 + \{\phi(l_1)\}^2 q^2}}$$

(∵ the law of conservation of energy

This equation is solved by Runge-Kutta method. Therefore, displacement of reed valve can be derived from this equation.

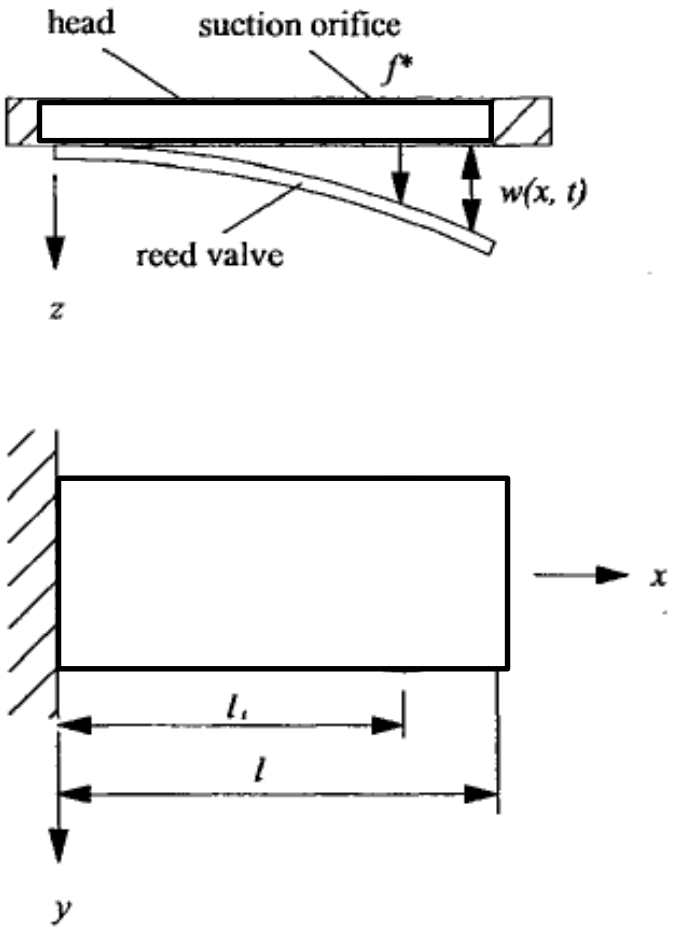

Figure 2.8. Model of reed valve dynamic analysis [12]

Finally, in order to response enough quickly, natural frequency of reed valve needs to be calculated and compared with pressure oscillation frequency. Figure 2.9. shows a pressure history at thrust wall. As shown in figure 2.9., the pressure oscillation frequency is about 200 Hz. Hence, if the natural frequency of reed valve were enough larger than 200 Hz, the reed valve can response enough quickly and can be used.

Therefore, the thickness of reed valve can be calculated by these three methods of design reed valve.

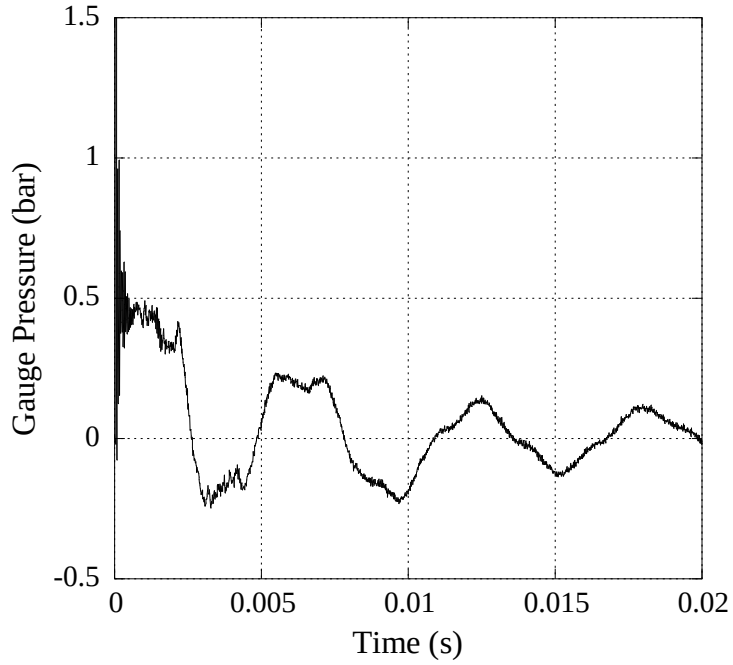

Figure 2.9. Pressure history at thrust wall

Chapter 3

Effect of Reed Valve Air-Breathing System

3.1 Factors Rerate to Thrust

In the recent study of our group, impulse measurement was conducted by Oda et al. They measured impulse I by integrating pressure at the closed end changing pulse duration time τ of microwave beam. In this experiment, they examined the relationship between pulse duration time τ and thruster length L. Impulse was increased with τ in short τ condition and hardly increased in long τ condition. It means that C_m decreases with long τ [13]. Momentum coupling coefficient C_m is energy conversion efficiency from average beam power P, pulse duration time τ and impulse I, and expressed as

$$C_m = \frac{I}{P \cdot \tau}$$

This phenomenon (decrement of impulse) happened when generated plasma length by pulse duration is longer than thruster length. Figure 3.1. shows relationship between pulse duration time and C_m. Here horizontal axis is expressed by normalized plasma length l which is defined as

$$l = \frac{U_{ioniz} \cdot \tau}{L}$$

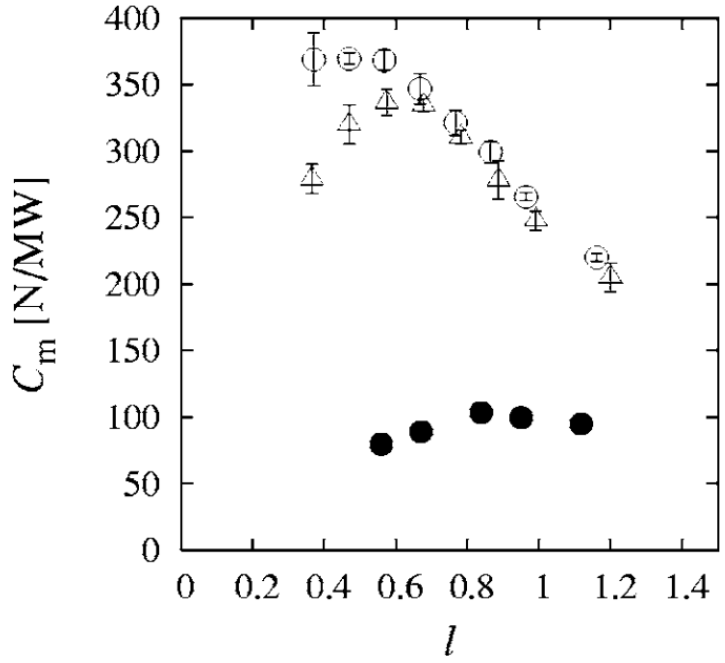

Figure 3.1. Relationship between C_m and normalized plasma length l. Reprinted from [13]

In this definition, U_{ioniz} is propagation velocity of ionization front of generated plasma. If this parameter is equal to unity, it means ionization front stopped propagating at the open end of the thruster. And figure 3.1. says there exists optimal l around 0.8 to maximize C_{m}. However, there is a possibility that optimal l changes with U_{ioniz}, for example depending on state of air inside the thruster.

Shiraishi et al. conducted experiment under multi-pulse condition with various repetitive frequency *f*. They showed that thrust is linearly related to *f* with air flow to refresh inside thruster [14]. In these experiments maximum *F* was a few N with sufficient air flow and less than 1 N without insufficient air flow.

Up here, it is clarified that thrust *F* is related to peak power P_{peak}, pulse duration time τ, repetitive frequency *f* and momentum coupling coefficient C_{m}. These relations can be summarized as,

$$F = P_{\mathrm{peak}} \cdot \tau \cdot f \cdot C_{\mathrm{m}}$$

However, there are some conditions C_{m} decreases like Figure 3.1. Oda et al. measured impulse-bit in multi-pulse operation. As Figure 3.2. shows, he found that impulse-bit after 2nd pulse is much lower than one by 1st pulse [15]. Therefore, it can be said that C_{m} decreases in multi-pulse operation. The reason for this is that the inside condition of second pulse is not same to it of first pulse.

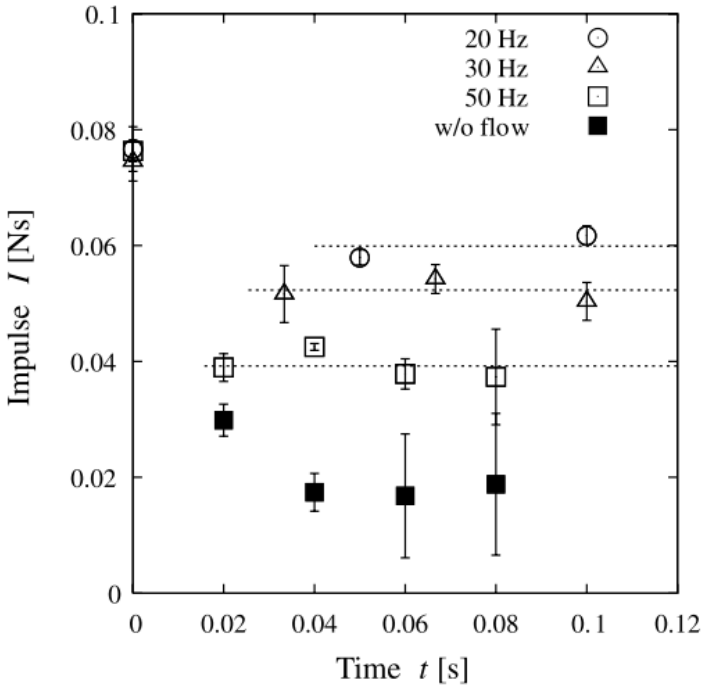

Figure 3.2. Impulse-bit decrement under multi-pulse operation reprinted from [15]

In addition, impulse is expressed as

$$I = A_{\text{thruster}} \cdot p_{\text{plateau}} \cdot t_{\text{plateau}}$$

In this formula, A_{thruster}, p_{plateau} and t_{plateau} are expressed cross sectional area of thruster, plateau pressure and plateau pressure maintained time, respectively. Figure 3.3. shows how to derive impulse from pressure history. As shown in this figure, the larger plateau pressure and plateau pressure maintained time, the larger impulse. In addition, thrust can be expressed as following.

$$F = I \cdot f$$

Therefore, it can be said that the larger plateau pressure and plateau pressure maintained time, the larger thrust.

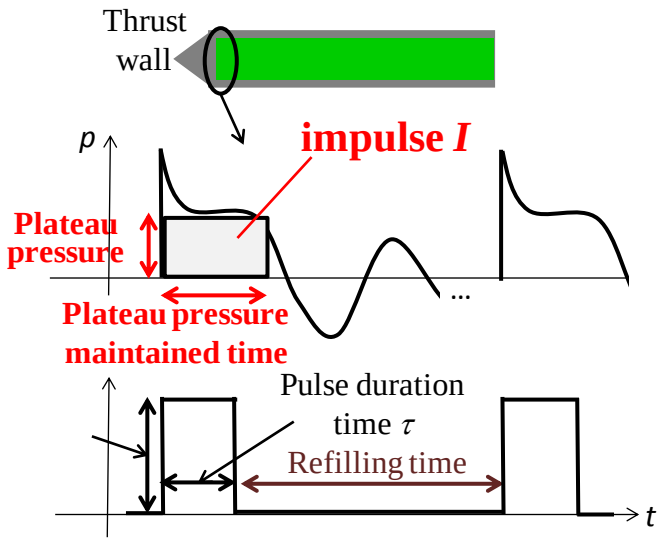

Figure 3.3. Pressure history at thrust wall (above) and signal history of microwave (bellow)

3.2 Objective of Present Experiment

In past study, impulse measurement experiment using thruster with reed valve under multi pulse operation was conducted by Komatsu et al. However, because shape of the thruster used this experiment was rectangular pipe, experimental data could not be compared with that of cylindrical pipe. In addition to this, because pulse count was operated at a maximum of 5 counts in this experiment, impulse data of large pulse count could not be obtained.

Therefore, cylindrical pipe thruster with reed valve is used and large pulse count is operated in present experiment. In addition, this experiment is conducted under high repetitive frequency in order to compare between thruster with reed valve and that of without reed valve under high repetitive frequency.

As mentioned above, objective of present experiment is to obtain effect of reed valve for impulse under large pulse count and high repetitive frequency operation. Furthermore, the objective is to know whether reed valve air-breathing system can be used in the future or not.

3.3 Experimental Apparatus

3.3.1 Experimental System

In this study, we conducted experiment twice. One is horizontal experiment used impulse stand. The other is vertical experiment used transmit and receive mirror system. Figure 3.4., figure 3.5. and figure 3.6. show conceptual schematic and picture of horizontal experiment. And, figure 3.7. and figure 3.8 show conceptual schematic and picture of vertical experiment.

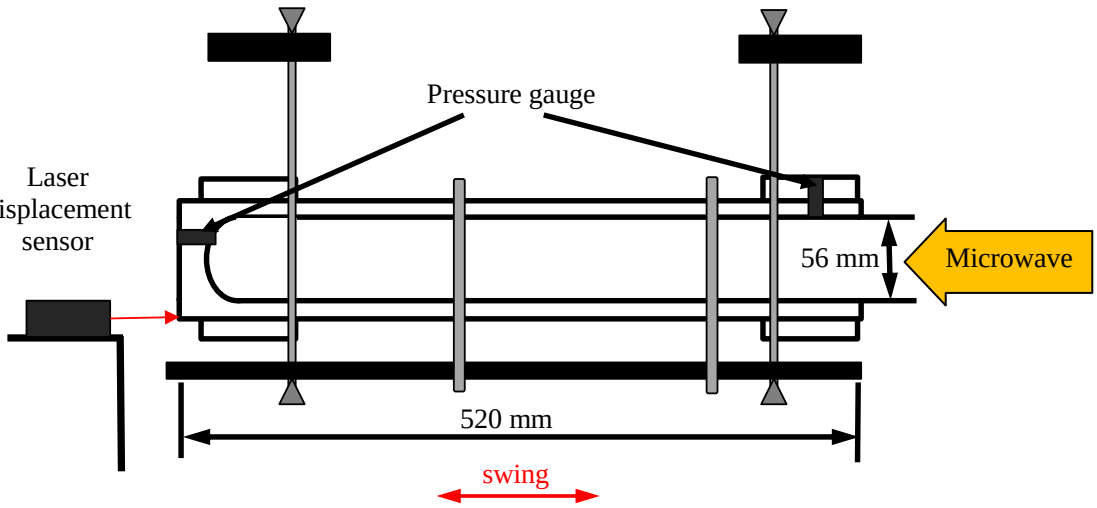

Figure 3.4. Conceptual schematic of horizontal experiment system

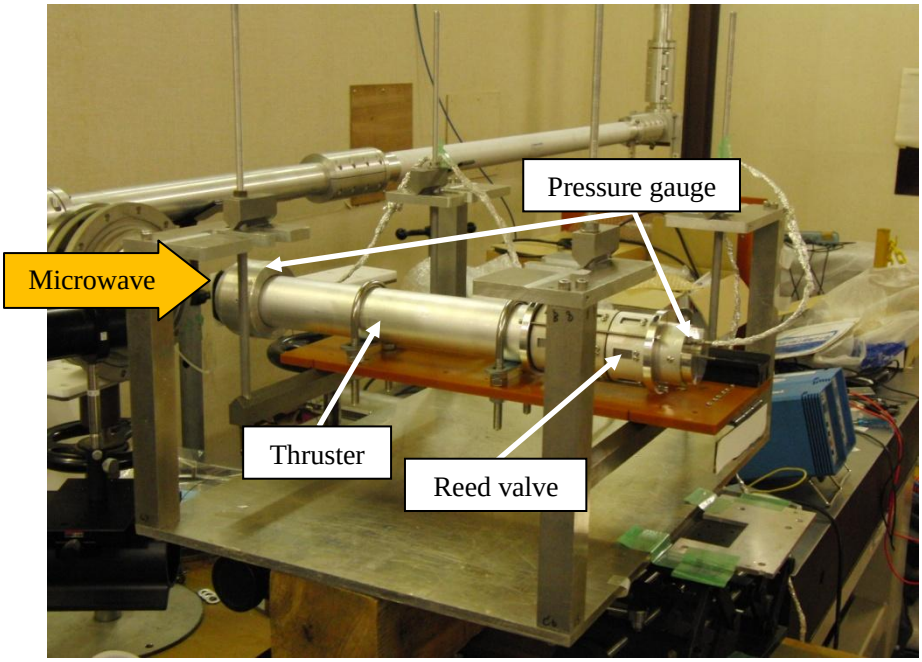

Figure 3.5. Picture of horizontal experimental system (took from side of the thruster)

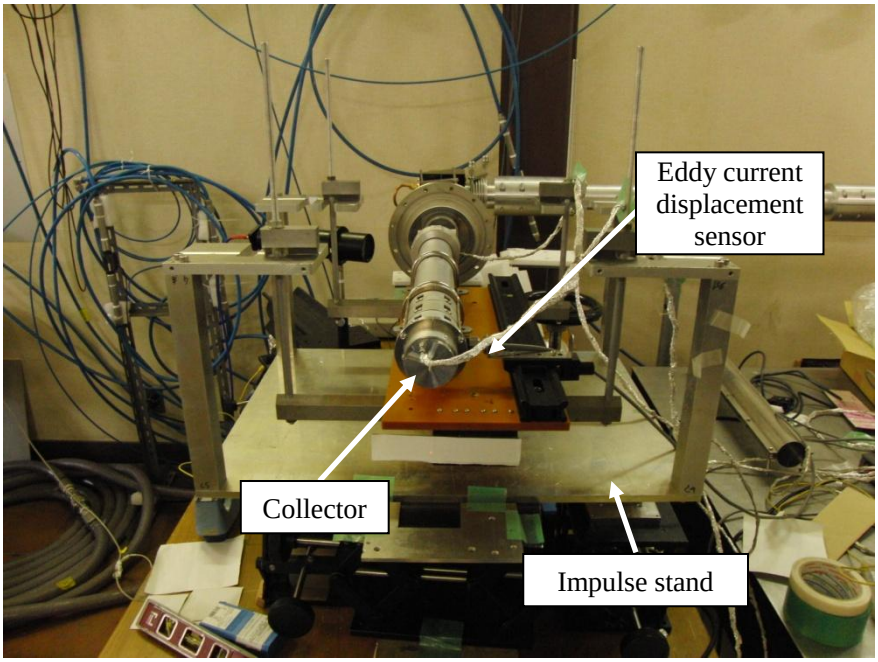

Figure 3.6. Picture of horizontal experiment (took from head of the thruster)

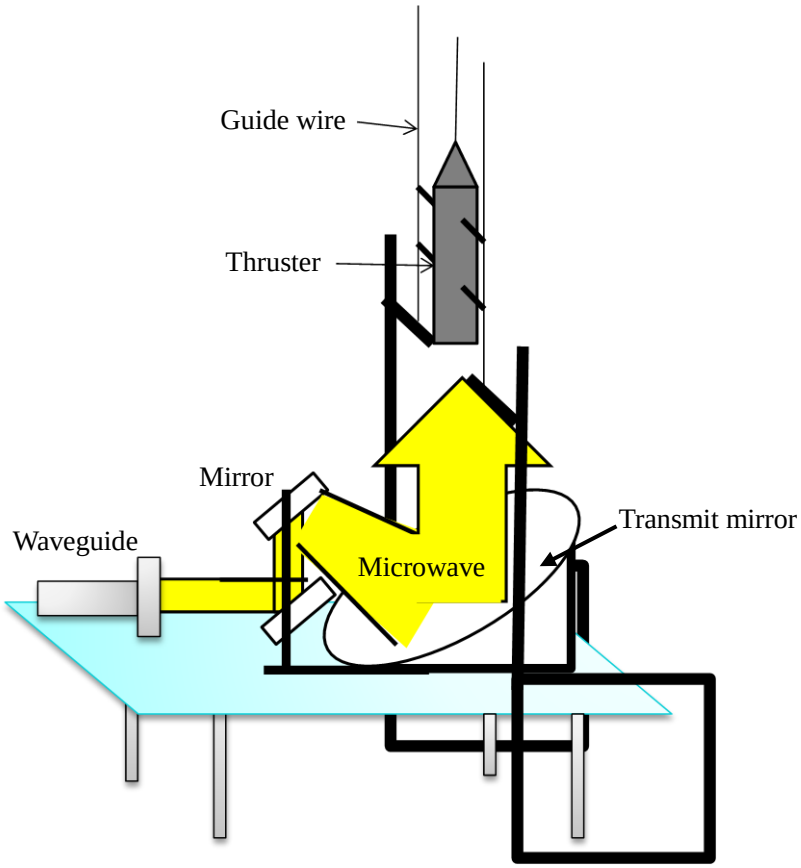

Figure 3.7. Conceptual schematic of vertical experiment system

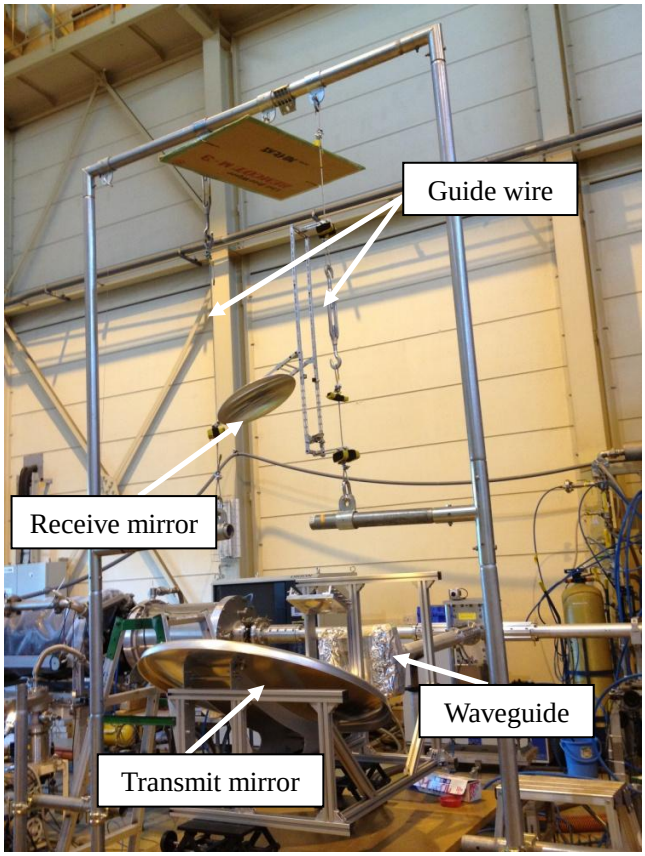

Figure 3.8. Picture of vertical experiment

In order to compare effect of reed valve, two thruster types were used in this experiment. First thruster type is no reed valve type thruster as shown in figure 3.9. The shape of this no reed valve thruster is cylindrical pipe. And this thruster is made of aluminum. As shown in figure 3.9., no reed valve thruster has acrylic window in order to observe plasma propagation inside the thruster. In addition to this, two screw holes are set at its collector and acrylic window so that pressure gauges are set. The second thruster type is with reed valve type thruster as shown in figure 3.10. and figure 3.11. In order to set reed valve at surface of cylindrical thruster, some short pipes are assembled with main body. Figure 3.10. shows a thruster with three reed valve parts. And figure 3.11. shows a thruster with six reed valve parts. As shown in figure 3.10. and figure 3.11., reed valves are assembled in a radial fashion. In addition, pressure gauge can be set at the collector of thruster with reed valve. Furthermore, we used reed valve made of SUS304CSP. Figure 3.12. shows detail of reed valve specification.

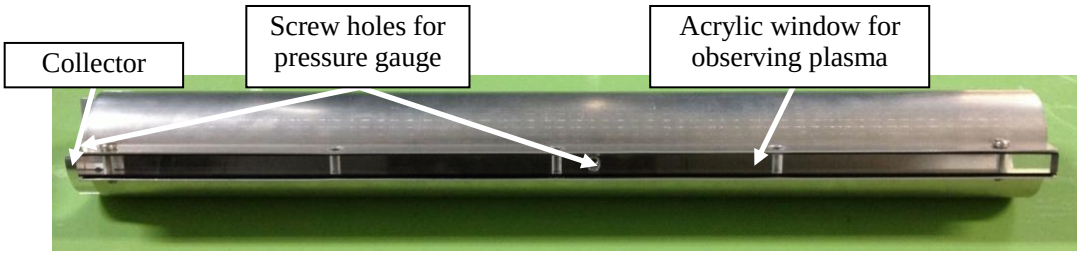

Figure 3.9. No reed valve type thruster

Figure 3.10. With reed valve type thruster (three pieces of reed valve part)

Figure 3.11. With reed valve type thruster (six pieces of reed valve part)

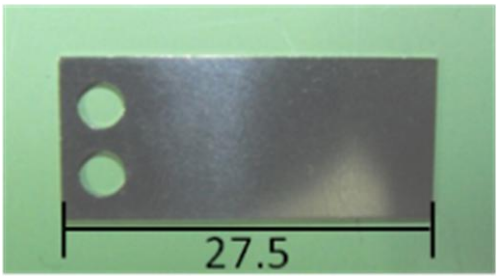

Material	: SUS304CSP
Length	: 27.5 mm
Width	: 12 mm
Thickness	: 0.2~0.3 mm
Natural Frequency	: about 400 Hz (0.2 mm)
	about 600 Hz (0.3 mm)

Figure 3.12. Specification of reed valve used in experiment

3.3.2 Measurement System

In this experiment, 3 sensors and high speed camera was used as measurement instruments. First, laser displacement sensor was used in order to measure amplitude of impulse stand. Second, pressure gauge was used in order to measure pressure inside the thruster. Furthermore, impulse and shock wave velocity was measured by pressure history. Third, eddy current displacement sensor was used in order to measure displacement of reed valve. In addition, high speed camera was used in order to observe plasma propagation inside the thruster. Each specification of measurement instruments are shown in figure 3.13. to figure 3.16.

Laser displacement sensor
for measurement of amplitude of impulse stand
Model number : KEYENCE LK-500
Sampling frequency : 1000 Hz
Range : ±250 mm
Resolution : 50 mm

Figure 3.13. Specification of laser displacement sensor

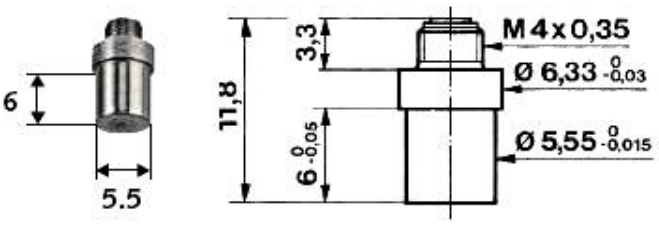

Pressure Gauge
for measurement of pressure
Model number : KISTLER 603B
Resonant frequency : 500 kHz
Range : 0~200 bar
Operating temperature : -196~200 ^{O}C

Figure 3.14. Specification of pressure gauge

Eddy Current Displacement Sensor
for measurement of displacement of reed valve
Model number : KEYENCE EX-422V
Sampling frequency : 40 kHz
Range : 0~10 mm
Response time : 0.075 ms (MAX)

Figure 3.15. Specification of eddy current displacement sensor

High speed camera
for observe plasma inside thruster
Model number : NAC MEMRECAM HX-1
Imaging element : 5 million
Flame rate : 50~1,300,0000 fps
Mass : about 9 kg

Figure 3.16. Specification of high speed camera

3.4 Result of Experiment

3.4.1 Effect of Reed Valve Air-Breathing System for Impulse

Figure 3.17. shows relationship between impulse of each thruster type and repetitive frequency. The error bars are drawn standard deviation and plots of no error bar are not enough data to draw error bar in this graph. In this graph, impulse of both without reed valve thruster and with reed valve thruster is almost constant until 200 Hz. However, impulse of without reed valve thruster decreases over about 200 Hz. The reason for this decrement is that hot air inside the thruster remains due to short refilling time (high repetitive frequency). Therefore, condition inside the thruster cannot return initial condition and C_m decrease drastically. By contrast, impulse of with reed valve thruster is almost constant until 250 Hz and decreases over about 250 Hz. The reason for this is that reed valve introduced fresh air and refilled inside thruster. Therefore, it is proved that reed valve air-breathing system contributes to increase of repetitive frequency. Besides, the gradient of impulse decrement over 200 Hz or 250 Hz is different each thruster type. The gradient of no reed valve thruster is smaller than that of with reed valve thruster. The reason for this is that once reed valve cannot response to pressure oscillation, reed valve prevents high pressure from being generated due to leak air. Therefore, reed valve has to be used in optimal repetitive frequency.

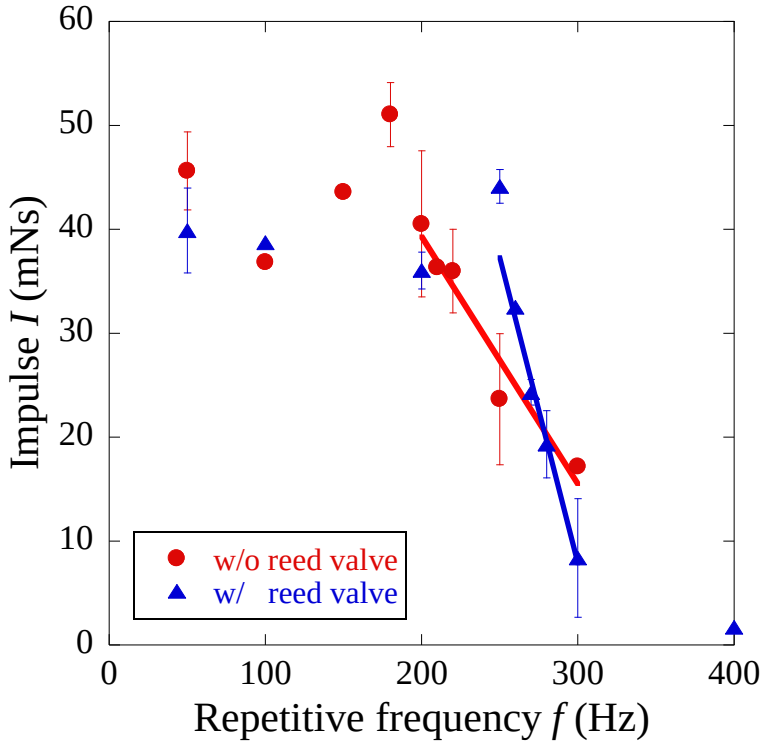

Figure 3.17. Relationship between impulse of each thruster and repetitive frequency (experimental condition: P = 570 kW, τ = 0.5 ms, 5th pulse, 3 pieces of reed valve part, thickness of reed valve is 0.2 mm)

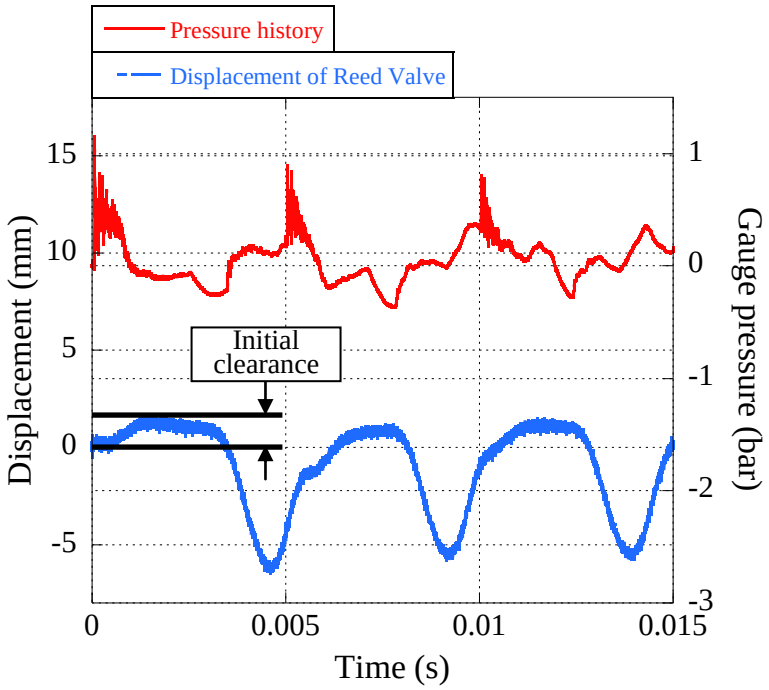

Figure 3.18. Initial clearance of reed valve (thickness of reed valve is 0.2 mm)

Table 3.1. Normalized 1st plateau pressure of each thickness

Thickness of reed valve	$p_{1plateau\_reed}$ / $p_{1plateau\_no\ reed}$
0.2 mm	0.72
0.3 mm	**0.96**

As mentioned at chapter 2.3, plastic deformation was occurred when thickness 0.2 mm reed valve was used. Figure 3.18. shows initial clearance of reed valve. Thereby, we redesigned and used thickness 0.3 mm reed valve in vertical experiment. Table 3.1. shows normalized 1st plateau pressure of each thickness of reed valve from vertical experimental data. As shown in table 3.1., there was leak of high pressure when thickness 0.2 mm reed valve was used. On the other hand, there was no leak of high pressure when thickness 0.3 mm reed valve was used. Therefore, plastic deformation was not occurred by redesign reed valve.

Figure 3.19. shows relationship between normalized plateau pressure and repetitive frequency. The normalized plateau pressure is measured at several dozen pulse count considered steady state. In other words, if this normalized plateau pressure equal 1, there is no thrust decrement. As shown in figure 3.19., normalized plateau pressure difference of each thruster type occurs at 50 Hz. Furthermore, maximum difference occurs over 100 Hz. The normalized plateau pressure of with reed

valve thruster is about twice larger than that of no reed valve thruster over 100 Hz. The reason for this is that reed valve introduced fresh air and refilled inside thruster same to horizontal experiment. In addition, the effect of reed valve for impulse occurs over 200 Hz in horizontal experiment. On the other hand, the effect of reed valve for impulse occurs over at least 50 Hz in vertical experiment. The pulse count was operated only 5 pulses in horizontal experiment. By contrast, the pulse count was operated several dozen pulses in vertical experiment. This is why, the difference of reed valve effect for impulse occurred each experiment.

As shown in figure 3.19., both p/p_1 of no reed valve thruster and p/p_1 of with reed valve thruster decreases at 100 Hz and 200 Hz. This decrement is due to pressure oscillation inside the thruster. Therefore, operation repetitive frequency has to be optimized in the future.

Therefore, the effect of reed valve for impulse is proved. However, there is room for improvement because p/p_1 of with reed valve thruster is not equal 1.

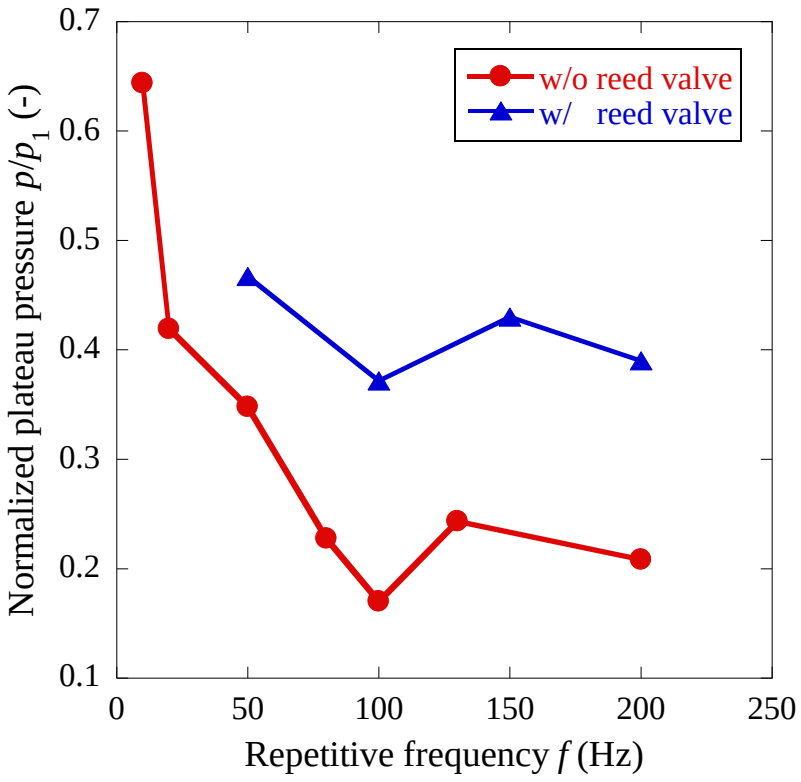

Figure 3.19. Relationship between normalized plateau pressure and repetitive frequency (experimental condition: P = 650 kW, several dozen pulse, 6 pieces of reed valve part, thickness of reed valve is 0.3 mm, used transmit mirror and receive mirror)

3.4.2 Discharge along the Way of the Thruster

As mentioned above chapter, we have already known that there is optimized length of plasma for C_m in past study. However, optimized plasma length cannot be maintained due to extending plasma length in multi pulse operation. In addition, plasma propagation inside aluminum thruster has never been observed in past study. Hence, we observed plasma propagation inside aluminum thruster in this experiment.

Figure 3.20. shows schematic of plasma propagation by high speed camera. Figure 3.21. and figure 3.22. are plasma propagation images taken through a side slot using a high speed camera at 1st pulse and 3rd pulse under 100 Hz operation and 400 Hz operation, respectively. And plasma propagation in these figures is printed frame-by-frame with the constant interval time. As shown in figure 3.21., a discharge occurs at collector when 1st pulse shot. However, another discharge, separate from the discharge at collector, occurs along the way of the thruster when 3rd pulse shot. Plasma propagates fast and the length of plasma gets long due to discharge along the way of the thruster. Furthermore, when the plasma length is longer than thruster length, high pressure inside the thruster will be short. This is why C_m cannot be maintained when the plasma length is longer than thruster length.

Besides, of course a discharge occurs at collector same to figure 3.21. when 1st pulse shot as shown in figure 3.22. However, some discharges, separate from the discharge at collector, occur along the way of the thruster when 3rd shot. In addition to this, the number of discharges increases compared with 100 Hz operation. Furthermore, the 3rd pulse plasma length of 400 Hz operation is longer than not only that of 100 Hz operation but also thruster length. In summary, the larger pulse count and repetitive frequency, the more the number of discharge.

The reason for the discharge along the way of the thruster is that electrons, generated 1st pulse, remain inside the thruster. Namely, discharges occur at the electrons remained inside the thruster when next microwave comes.

Therefore, we have to exhaust the electrons in order to prevent discharge along the way of the thruster. Hence, reed valve air-breathing system can be used to create flow and exhaust the electrons in the future.

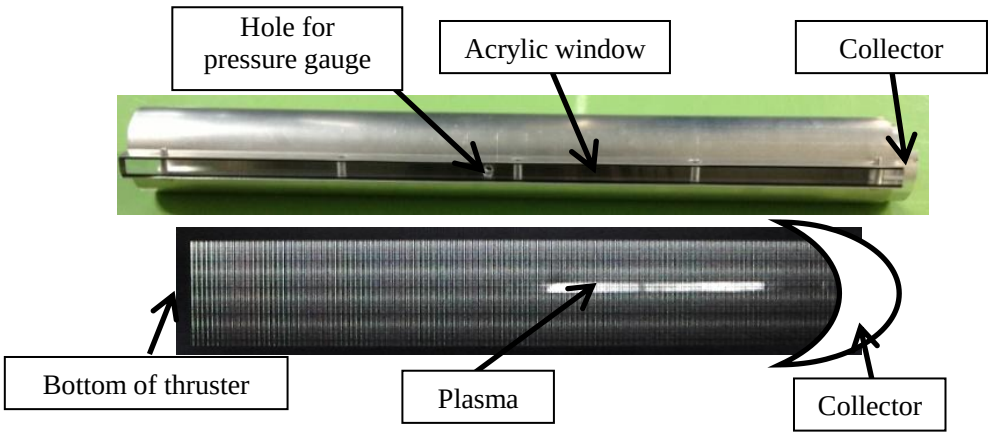

Figure 3.20. Schematic of plasma propagation

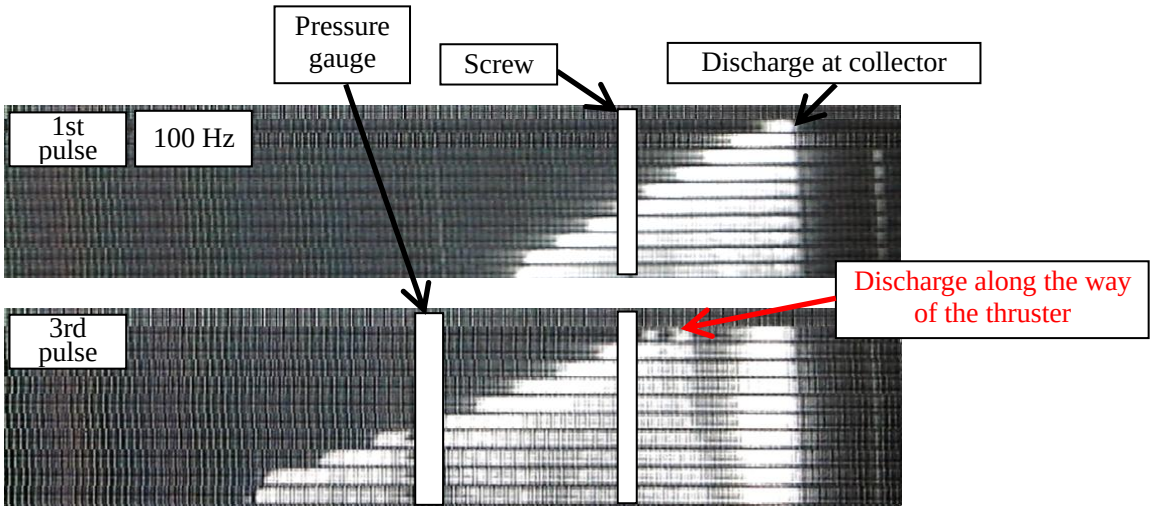

Figure 3.21. Plasma emission images taken through a side slot using a high speed camera at 1st pulse and 3rd pulse under 100 Hz operation (experimental condition: P = 570 kW, τ = 0.5 ms, frame-by-frame with the constant time interval)

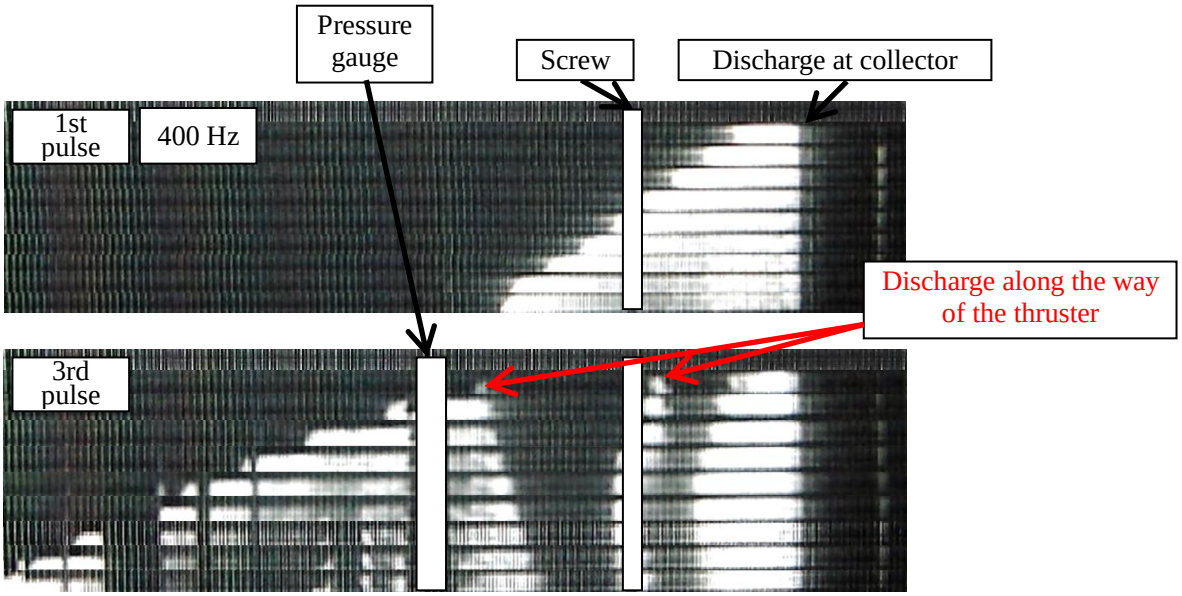

Figure 3.22. Plasma emission images taken through a side slot using a high speed camera at 1st pulse and 3rd pulse under 400 Hz operation (experimental condition: P = 570 kW, τ = 0.5 ms, frame-by-frame with the constant time interval)

Chapter 4

Next Microwave Rocket Thruster

4.1 Next Trends of Microwave Rocket Thruster

Figure 4.1. shows relationship between momentum coupling coefficient C_m and repetitive frequency of each pulse duration time. As mentioned above chapter, there is optimized length of plasma which is determined by pulse duration time mainly. However, plasma length could not be maintained optimized length under multi pulse operation in past study. As shown in figure 4.1., C_m can be maintained until about 250 Hz operation by reed valve air-breathing system. However, C_m of large pulse duration time τ is quite larger than that of small pulse duration time τ. Hence, although reed valve air-breathing system contributes impulse, C_m cannot be maintained large condition by using only reed valve air-breathing system. Therefore, optimized pulse duration time has to be maintained by other device.

As mentioned above, C_m will decrease when the plasma length is larger than thruster length. Therefore, it is suggested that thruster length should be extended optimized length. If same size and material thruster (inside diameter: 56 mm, thickness: 2 mm, material: aluminum) were used in the future, we have to know simply relationship between thruster length and thrust in order to design new thruster.

Firstly, influence of extend thruster for thrust is about 0.96 N per 100 mm because thruster weight is about 100 g per 10 mm.

Secondly, plasma length is about 500 mm per τ = 1.0 ms in this experimental condition. On the other hand, pulse duration time is about 0.2 ms per 100 mm.

Thirdly, influence of increase pulse duration time for thrust is about 18 N per τ = 1.0 ms in this experimental condition if peak power of microwave, C_m and repetitive frequency were constant.

Therefore, if peak power of microwave, C_m and repetitive frequency were constant, the effect of extend thruster for thrust is about 3.6 N per 100 mm extend thruster. However, we should conduct experiment for extend thruster in the future because this estimation is no more than an estimation.

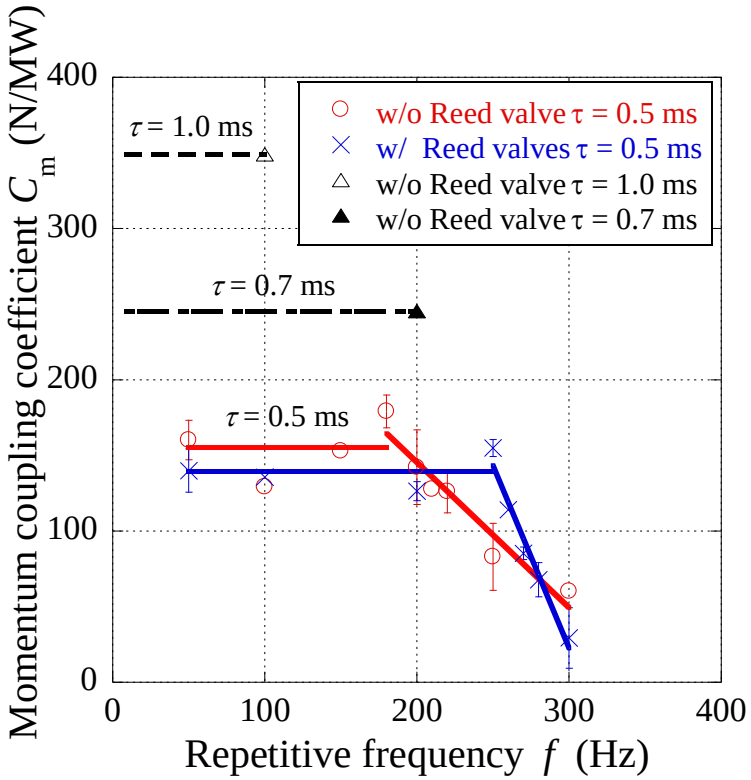

Figure 4.1. Relationship between momentum coupling coefficient C_m and repetitive frequency f of each Pulse Duration Time τ (experimental condition: P = 570 kW, 5th pulse, 3 pieces of reed valve part, thickness of reed valve is 0.2 mm)

4.2 Next Trends of Reed Valve Air-breathing System

4.2.1 The number of Reed Valve

As mentioned above, the effect of reed valve air-breathing system was proved in this experiment. Which direction should we choose increase or decrease the number of reed valve? The answer is following figures 4.2. Figure 4.2. shows relationship between normalized plateau pressure maintained time $t_{plateau}$ / $t_{1st\ plateau}$ and pulse count of no reed valve type thruster. Figure 4.3. and figure 4.4. also shows relationship between normalized plateau pressure maintained time and pulse count of 3 pieces and 6 pieces of reed valve part type thruster, respectively. Here, normalized plateau pressure maintained time expresses proportion of plateau pressure maintained time to that of 1st pulse. Namely, when this proportion is equal one, shock wave velocity does not increase. In other words, the temperature inside the thruster does not increase. Furthermore, it can be said that the air inside the thruster is refilled well.

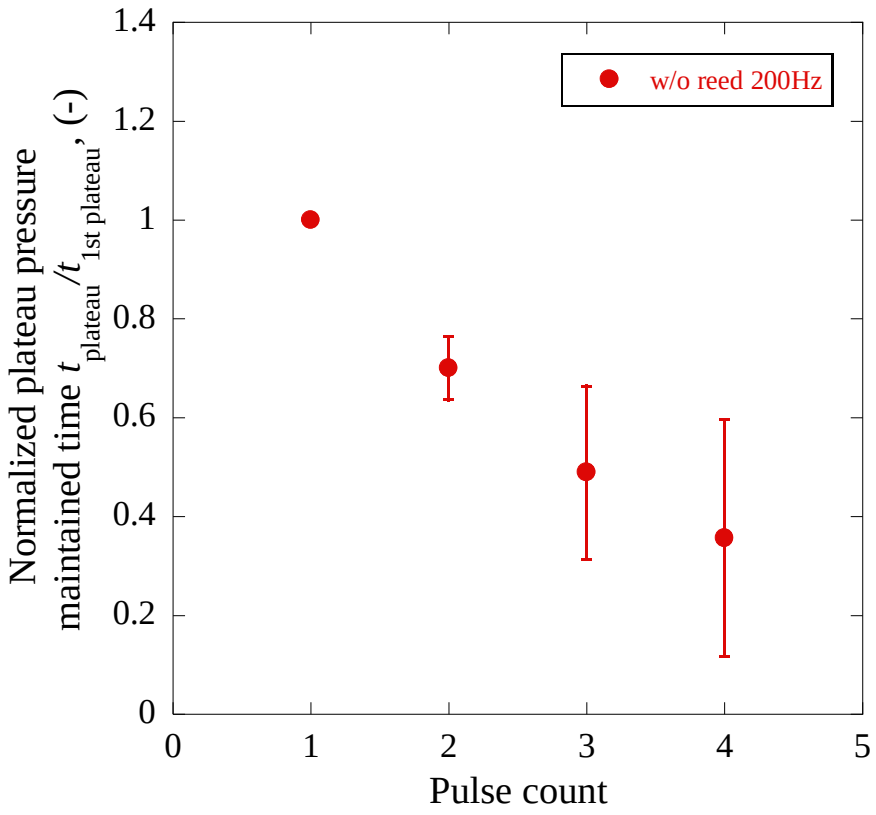

Figure 4.2. Relationship between normalized plateau pressure maintained time and pulse count of no reed valve type thruster

Firstly, the larger pulse count and repetitive frequency, the smaller $t_{plateau}$ / $t_{plateau1}$ as shown in figure 4.2. The reason for this is that the temperature of air inside the thruster increases due to small refilling. On the other hand, $t_{plateau}$ / $t_{plateau1}$ of 3 pieces reed valve part type thruster is larger than that of no reed valve type thruster as shown in figure 4.3. Of course, the reason for this is that reed valve contributes refill air inside the thruster. Furthermore, $t_{plateau}$ / $t_{plateau1}$ of 6 pieces reed valve part type thruster is larger than that of no reed valve type thruster as shown in figure 4.4. Therefore, 6 pieces of reed valve part type thruster can refill well than 3 pieces of reed valve part type thruster.

In summary, we should choose the direction of reed valve in the future, which is increase the number of reed valve. Therefore, we need to conduct further experiment in order to optimize the number of reed valve in the future.

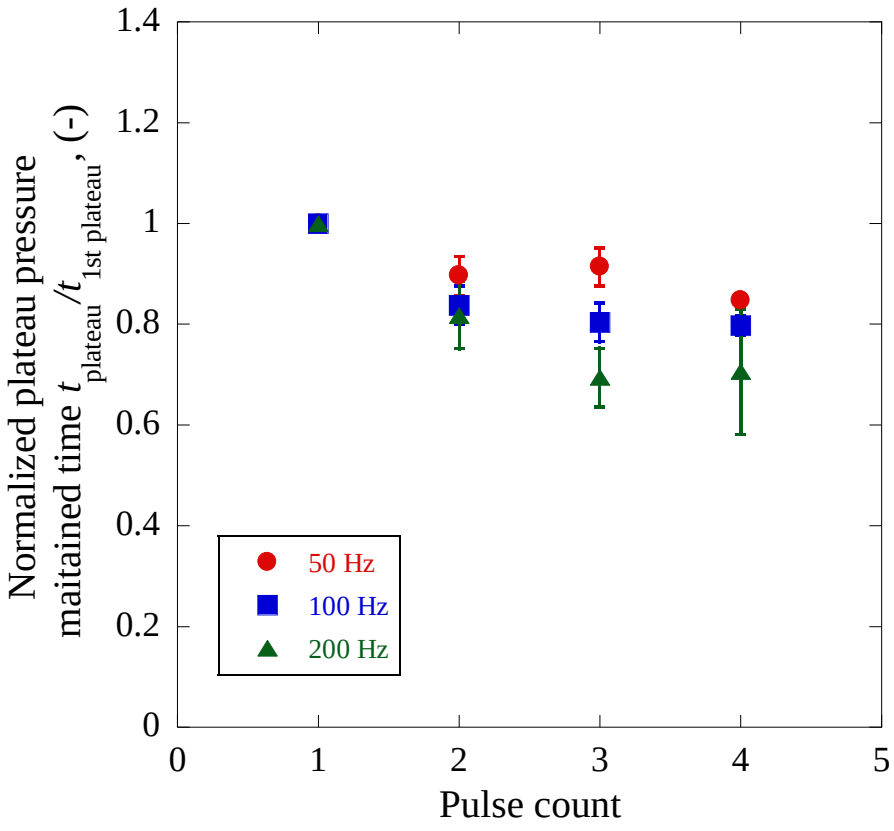

Figure 4.3. Relationship between normalized plateau pressure maintained time and pulse count of 3 pieces of reed valve part type thruster

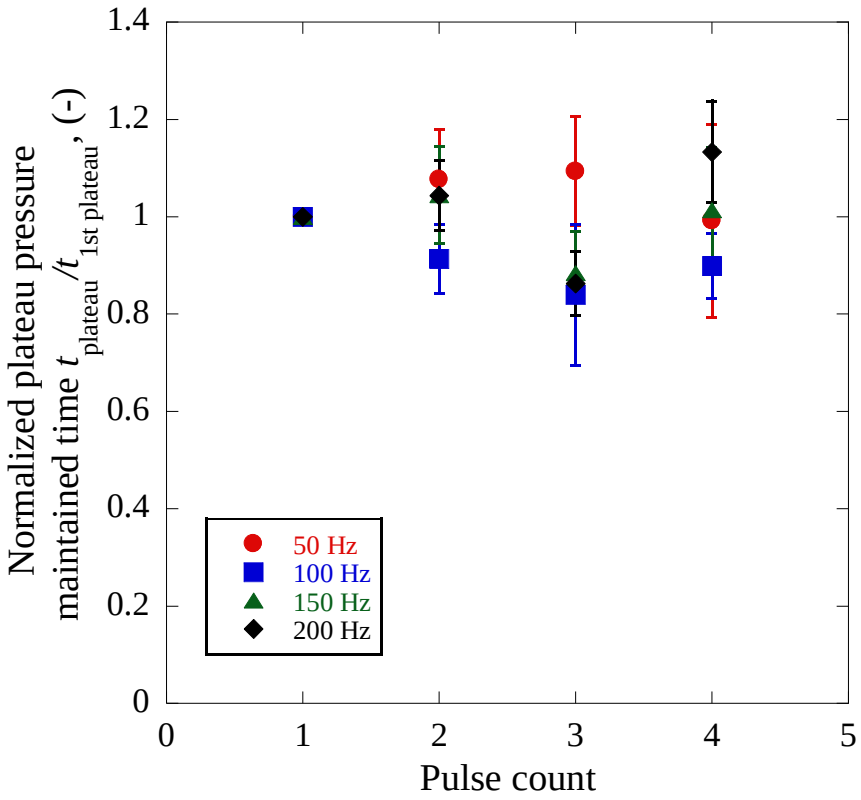

Figure 4.4. Relationship between normalized plateau pressure maintained time and pulse count of 6 pieces of reed valve part type thruster

4.2.2 Material of Reed Valve

We used SUS304CSP as material of reed valve in this experiment. However, the material of reed valve needs to be considered new material for further improvement performance of reed valve. Hence, we estimated the performance of reed valve made of CFRP (Carbon Fiber Reinforced Plastic) by conducting design calculation. The design calculation method is dynamic analysis mentioned at chapter 2.3 Design of Reed Valve. Figure 4.5. shows reed valve made of CFRP.

Generally, reed valves made of CFRP is used for high performance 2 cycle engine. The reason for this is that the reed valve made of CFRP has high natural frequency and strength. In other words, the reed valve made of CFRP responses quite quickly to pressure oscillation. This is why we chose CFRP as reed valve material.

Figure 4.6. and figure 4.7. show result of this calculation. Figure 4.6. expresses displacement at head of reed valve and pressure oscillation from experiment. Figure 4.7. expresses displacement of reed valve each time. In addition, this displacement is seen from the side of reed valve.

As shown in figure 4.6., reed valve made of CFRP can response to pressure oscillation enough quickly. In addition to this, maximum displacement is about 6 mm. This displacement is larger than that of reed valve made of SUS304CSP (4 mm). Besides, natural frequency of reed valve made of CFRP is 1100 Hz and it is quite larger than that of SUS304CSP (600 Hz). In addition, maximum moment of reed valve made of CFRP is 0.16 Nm. It is larger than break moment (FS = 1.2).

As shown in figure 4.7., the reed valve made of CFRP moves in first-order mode. Therefore, reed valve made of CFRP can close and seal in order to prevent leak of high pressure.

Therefore, it can be said that the performance of CFRP is superior to that of SUS304CSP.

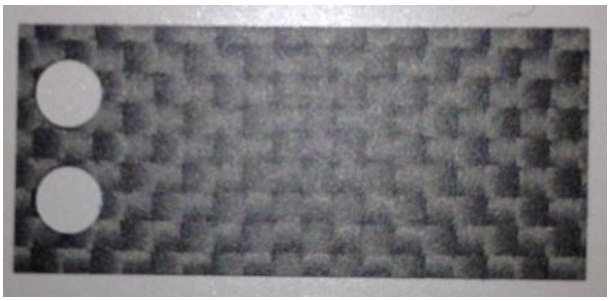

Figure 4.5. Reed valve made of CFRP

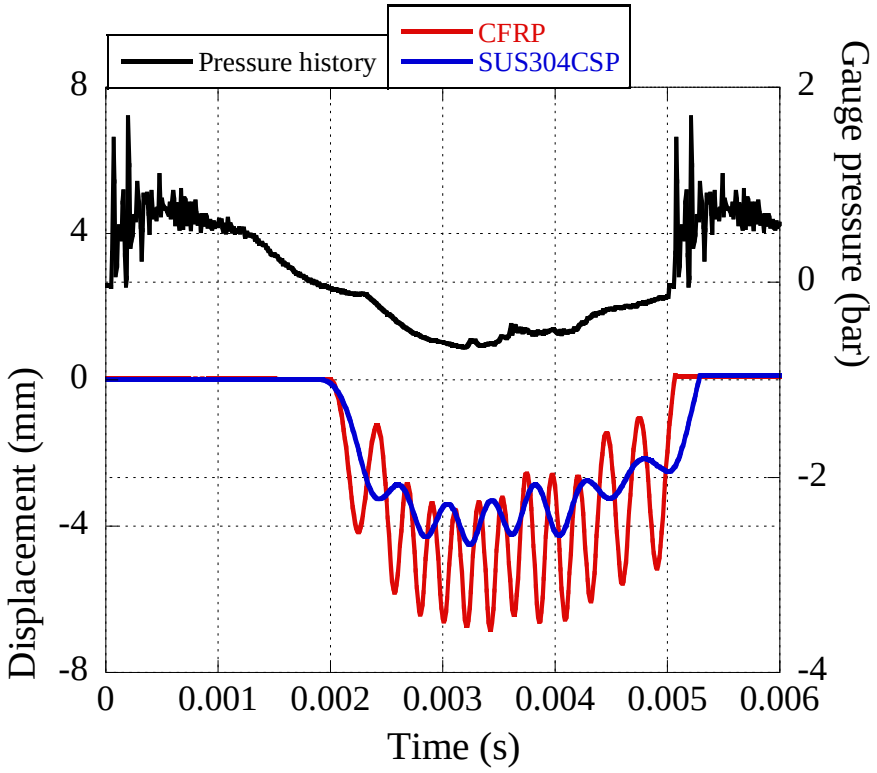

Figure 4.6. Displacement result at head of reed valve by design calculation

(material: CFRP and SUS304CSP, thickness: 0.3 mm, natural frequency of reed valve: 1100 Hz (CFRP) and 600 Hz (SUS304CSP), maximum moment: 0.16 Nm (CFRP) and 0.162 Nm (SUS304CSP), break moment: 0.17 Nm (CFRP) and 0.19 Nm (SUS304CSP) (FS = 1.2), frequency of pressure oscillation: 200 Hz)

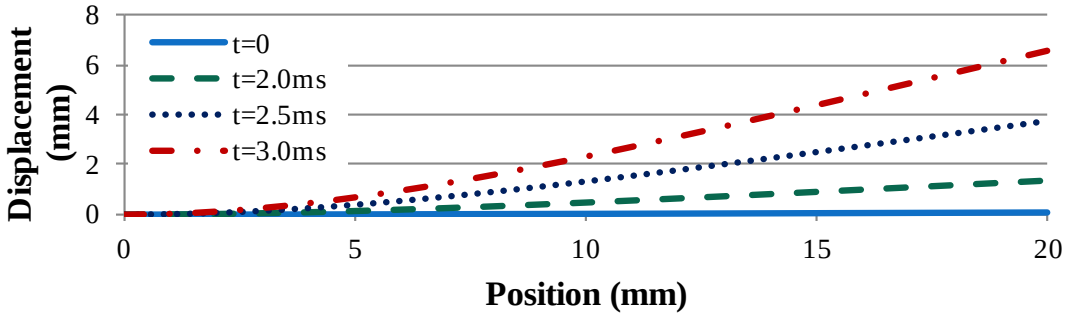

Figure 4.7. Displacement result each position of reed valve design calculation

(the Material is CFRP, frequency of pressure oscillation is 200 Hz)

Meanwhile, CFRP is characterized by low heat resistance. Reed valve for microwave rocket needs heat resistance because air inside the thruster is heated to several hundred degrees Celsius. There is a simple test to check for low heat resistance. The test is to heat reed valve by a lighter. Figure 4.8. shows reed valve made of CFRP heated by a lighter. As shown in this figure, reed valve is burned. Therefore, CFRP cannot be used for reed valve of microwave rocket because of its low heat resistance. However, if CFRP could be tolerant of heat, CFRP can be best material for reed valve of microwave rocket.

In summary, we have to develop CFRP coated by some heat resistance material in order to use CFRP reed valve in the future.

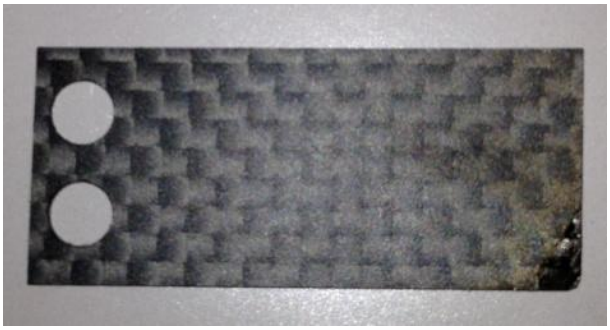

Figure 4.8. Burned CFRP reed valve

Chapter 5
Conclusion

5.1 Effect of Reed Valve Air-Breathing System

In this study, reed valve was redesigned and used experiment. Effect of reed valve for impulse is proved. Namely, the range of operation repetitive frequency is extended by introducing reed valve air-breathing system. In addition, decrement of impulse was prevented by reed valve. In other words, normalized plateau pressure of with reed valve type thruster can be maintained twice larger than that of no reed valve type thruster. However, because the normalized plateau pressure is not equal one, there is a room for improvement reed valve. Besides, it was found that reed valve can refill and cool air inside the thruster. In summary, it can be said that reed valve air-breathing system can be used for microwave rocket in the future.

5.2 Next Microwave Rocket Thruster

It was found that optimized plasma length cannot be maintained due to discharges along the way of the thruster. Therefore, the direction, we should choose, is determined to extend the length of thruster. However, discharges along the way of the thruster needs to be prevented by increasing the number of reed valve attached the thruster in the future. Effect of reed valve is proved, but the material of reed valve has to be changed and improve the performance because there is a room for improvement it. Therefore, CFRP was evaluated by calculation in this study. As a result, it was found that CFRP is superior to SUS304CSP. However, CFRP is characterized by low heat resistance. Therefore, we have to develop CFRP coated by some heat resistance material in order to use CFRP reed valve in the future.

References

[1] Koelle,D., “Specific transportation costs to GEO-past, present and future”, *Acta Astronautica*,53, 797-803, **2003**

[2] Saito, Y.; Yamashiro, R. & Ohkubo, S., “The Vision for Next Flagship Launch Vehicle of Japan”,*The 26th International Symposium on Space Technology and Science*, **2008**

[3] Kantrowaitz,A., “Propulsion to Orbit by Ground-Based Lasers”, *Astronautics and Aeronautics*, 10, 74, **1972**

[4] L. N. Myrabo, “World record flights of beamed-riding rocket light craft”, *American Institute of Aeronautics and Astronautics Paper N*, pp. 2001-3798, **2001**

[5] J. P. Knecht and M. M. Micci, “Analysis of Microwave-heated planar propagating hydrogen plasma” *AIAA Journal*, 26(2), pp188-194, **1988**

[6] Y. Oda., K. Komurasaki, K. Takahashi, A. Kasugai, and K. Sakamoto, “Plasma generation using high-power millimeter wave beam and its application for thrust generation”, *J. App. Phys. 100*, **2006**

[7] Y. Shiraishi, Y. Oda, T. Shibata, K. Komurasaki, K. Takahashi, A. Kasugai and K. Sakamoto, “Air Breathing Processes in a Repetitively Pulsed Microwave Rocket”, *AIAA Paper*, **2008**

[8] Y. Oda, T. Shibata, K. Komurasaki, K. Takahashi, A. Kasugai and K. Sakamoto, “Thrust Performance of a Microwave Rocket Under Repetitive-Pulse Operation”, *J. Propulsion and Power 25(1)*, pp118-122, **2009**

[9] K. Sakamoto, A. Kasugai, K. Takahashi, R. Minami, N. Kobayashi and K. Kajiwara, “Achievement of robust high-efficiency 1MW oscillation in the hard-self-excitation region by a 170GHz continuous-wave gyrotron”, *Nature Physics*, Vol.3, No.6, pp.411-414, **2007**

[10] M. Fukunari, T. Yamaguchi, R. Komatsu, H. Katsurayama, K. Komurasaki and Y. Arakawa, “Preliminary Study on Microwave Rocket Engine Cycle”, *Plasma Application and Hybrid Functionally Materials*, 20, 75, **2011**

[11] T. Endo, J. Kasahara, A. Matsuo, K. Ibara, S. Sato and T. Fujiwara, “Pressure history at the closed end of a simplified pulse detonation engine”, *AIAA journal*, 42, pp. 1921-1930, **2004**

[12] H. C. Sheu and Y.Z.R.Hu, “Nonlinear Vibration Analysis of Reed Valves”, *International Compressor Engineering Conference paper*, 1419, **2000**

[13] Y. Oda, T. Shibata, K. Komurasaki, K. Takahashi, A. Kasugai and K. Sakamoto, ”Thrust Performance of a Microwave Rocket Under Repetitive-Pulse Operation”, *JOURNAL OF PROPULSION AND POWER*, *25*, 118-122, **2009**

[14] Y. Shiraishi, Y. Oda, T. Shibata, K. Komurasaki, K. Takahashi, A. Kasugai and K. Sakamoto, “Air Breathing Processes in a Repetitively Pulsed Microwave Rocket”, *AIAA-2008-1085, 46th AIAA Aerospace Sciences Meeting and Exhibit, Reno, Nevada, Jan. 7-10*, 1085, **2008**

[15] Y. Oda, K. Komurasaki, K. Takahashi, A. Kasugai, and K. Sakamoto, "An Experimental Study on a Thrust Generation Model for Microwave Beamed Energy Propulsion", *AIAA-2006-765, 44th AIAA Aerospace Sciences Meeting and Exhibit, Reno, Nevada, Jan. 9-12,* **2006**

修士論文に関する発表等一覧

(1) 投稿論文 1 件 (共著 1 件)

1) 小松怜史、山口敏和、小田靖久、**齋藤翔平**、福成雅史、小紫公也、梶原健、高橋幸司、坂本慶司、“大電力・高デューディ比作動によるマイクロ波ロケットの推力向上”、日本航空宇宙学会論文集、Vol. 60、No. 6、pp. 235-237、2012 年 12 月

(2) 国内学会における発表 5 件 (筆頭著者 3 件, 共著 2 件)

1) **齋藤翔平**、小松怜史、山口敏和、小紫公也（東京大学)、小田靖久、坂本慶司（JAEA）“マイクロ波ロケットにおけるリードバルブの応答性評価”、第 55 回宇宙科学技術連合講演会、2M06、 松山、 2011 年 12 月
2) **齋藤翔平**、小松怜史、福成雅史、山口敏和、小紫公也（東大)、小田靖久、梶原健、高橋幸司、坂本慶司（JAEA）“マイクロ波ロケット高周波作動時の吸気性能評価とリード弁による効果の検証”、平成 23 年度衝撃波シンポジウム、178、柏、2012 年 3 月
3) **齋藤翔平**、浅井健太、栗田哲志、福成雅史、山口敏和、小紫公也（東大)、小田靖久、梶原健､高橋幸司､坂本慶司(JAEA)“kg 級マイクロ波ロケットの打上げ実証実験報告”、平成 24 年度宇宙輸送シンポジウム、STEP-2012-034、相模原、2013 年 1 月
4) 栗田哲志、**齋藤翔平**、福成雅史、山口敏和、小紫公也（東京大学)、小田靖久、梶原健、高橋幸司､坂本慶司(JAEA)､“マイクロ波ロケットの繰返しパルス周波数限界の向上”、第 56 回宇宙科学技術連合講演会、P35、別府、2012 年 11 月
5) 小松怜史、**齋藤翔平**、福成雅史、山口敏和、小紫公也（東京大学)、小田靖久、梶原健、高橋幸司、坂本慶司（JAEA)、“マイクロ波ロケットにおけるリードバルブ式吸気機構の推力への影響”、平成 23 年度宇宙輸送シンポジウム、STCP-2011-078、相模原、2012 年 1 月

(3) 国際会議における発表 1 件 (筆頭著者 1 件)

1) **Shohei Saitoh**, Reiji Komatsu, Toshikazu Yamaguchi, Kimiya Komurasaki (The University of Tokyo), Yasuhisa Oda, Ken Kajiwara, Koji Takahashi, Keishi Sakamoto (Japan Atomic Energy Agency), “Microwave Rocket with 30N thrust and further thrust augmentation with reed-valve air intake”, *The 8th IEEE Vehicle Power and Propulsion Conference (VPPC 2012)*, SS01-0290, Seoul, Oct. 2012